The Effect of Crystallographic Texture on the Wrap Bendability in AA5754-O Temper Sheet Alloy

Haiou Jin, Yihai Shi and Alok K. Gupta

Novelis Global Technology Centre, P.O. Box 8400, Kingston, Ontario, CANADA K7L 5L9

Commercial AA5754-O temper (fully annealed condition) sheet product is used for a variety of automotive inner and structural panel applications. It has been reported that a strong $\{001\}\langle100\rangle$ cube crystallographic texture in Al-Si-Mg-(Cu) alloys has a positive effect on the sheet formability, although less is known of such effect in Al-Mg alloys. In the present work, the effect of cube texture on the bendability of AA5754 alloy is examined. Two AA5754 ingots were homogenized and rolled via different processing routes with the aim to produce one product with weak texture and another with a strong cube texture. The grain structure, texture, tensile properties and bendability were characterized by optical microscopy, scanning electron microscopy (SEM), electron backscatter diffraction (EBSD) in SEM, X-ray diffraction, tensile and wrap bendability testing. It has been demonstrated that the high-cube sheet has better bendability than the low-cube one. This phenomenon is explained by the fact that the cube texture significantly reduces the strain localization under in-plane plane strain tension.

Keywords: Al-Mg alloy, AA5754, cube texture, bendability.

1. Introduction

Al-Mg (5XXX) and Al-Si-Mg-(Cu) (6XXX) alloys have been increasingly used in automobile body applications to replace the conventional steels [1]. However, the formability of aluminum alloys is inferior by comparison, thus any improvement of formability in aluminum alloy sheets has significant commercial ramifications. Crystallographic texture is one of the factors that affect the sheet formability. Most of the 5XXX and 6XXX aluminum sheet alloys supplied to automotive industry are of fully annealed conditions, where the cube is a characteristic texture component. A strong cube texture in sheet metal leads to high planar anisotropy and low r-value [2], but it has also been found that the formability, especially the tensile elongation and bendability, could be improved in some aluminum alloys, such as AA6XXX [3]. The r-value represents the width-to-thickness reduction ratio in a uniaxial tensile test.

Al-Mg sheet alloy AA5754 supplied in O-temper has been widely used as automotive inner and structural panels. Since these panels are formed by bending and hemming, the bendability is extremely important for this application. To investigate the possibility of improving the bendability in AA5754 by an increased cube texture, in the present work two AA5754 ingots were homogenized and rolled with different processing routes, leading to one with low and another with high cube texture component. The grain structure, texture, tensile properties and bendability were characterized by optical microscopy, SEM, EBSD in SEM, X-ray diffraction, tensile and wrap bend testing. The effect of texture on sheet formability was studied by rate-dependent crystal plasticity model, and the correlation between the bendability and texture will be discussed.

2. Experiments

Two 2.6mm thick AA5754 sheets, labeled Sheet-L and Sheet-H with nominal composition of Al-3Mg-0.3Mn-0.2Fe (wt.%), were fabricated through different rolling processes from DC ingots to achieve similar grain structure but different crystallographic textures. The grain structure was examined in the sheet longitudinal section under optical microscope, and the mean grain sizes were

measured by the line intercept method. The crystallographic textures were determined using X-ray diffraction technique in the surface, one-quarter thickness and centre in a Rigaku X-ray machine with a radiation source of RU-200B rotating anode and Cr target, and analysed by Van Houtte's MTM-FHM software [4]. The grain structure and texture were also investigated by EBSD on the longitudinal section through the sheet thickness, using a Phillips XL30S field emission gun (FEG) SEM equipped with a Nordlys II detector. The EBSD maps were 10mm in the rolling direction (RD) and 2.6mm in the thickness direction with a step size of 10μm, and the data acquisition and subsequent analyses were done by HKL Channel 5 software.

Tensile testing was done in standard ASTM tensile specimens (2 inch gauge length and 0.5 inch gauge width) in the longitudinal and transverse directions, i.e., 0° and 90° to the RD. The bending performance was examined using the wrap bend test method, while the specimens were wrapped around mandrels with different radii. The bendability is quantified by a parameter $\frac{r}{t}$, where r is the minimum radius of mandrel that the specimen can pass without cracks and t is the specimen thickness, and a lower $\frac{r}{t}$ value indicates better bendability. In the present work, the bending specimens were prepared in both the longitudinal and transverse directions, and some specimens were pre-strained by stretching in a tensile machine to 18% elongation. To investigate the formation of strain localization upon forming, two standard tensile specimens were prepared in the transverse direction, with one side of the gauge area carefully ground and electro-polished. The specific tensile specimens were pre-strained by stretching to 18% elongation, then the electro-polished gauge parts were cut off, and the microstructure and surface topography were examined in the SEM.

To further elucidate the influence of initial texture on the strain localization that eventually leads to localized necking, a Finite Element (FE) based rate-dependent single crystal plasticity model has been used and implemented into ABAQUS [5] as a user subroutine in the analysis. A total of 30% tensile elongation was applied along the RD, while the approach in detail can be found in [6]. The initial averaged texture of the sheet, directly generated from the EBSD maps, has been applied to a region about 5.01 mm in length (rolling) by 2.55 mm in width (transverse) in the model. A 2×2 element per grain was used for the mesh density resulting in 5μm per element. The values for the material parameters in the crystal plasticity are obtained through fitting the measured tensile curves. It should be emphasized that the main purpose of this FE analysis is to study the influence of the cube texture on the localized necking during elongation, and the overall conclusions are not particularly dependent on the values of the material parameters.

3. Results and Discussion

The two sheets are fully recrystallized with relatively equi-axed grain shape (Fig. 1), but the grain size in Sheet-L is slightly coarser than Sheet-H (Table 1). In addition, there is no obvious difference on the particle size and particle spatial distribution between the two sheets (Fig. 2). The (111) X-ray pole figures are shown in Fig. 3, clearly indicating that Sheet-H has much stronger cube texture and severer through-thickness texture variation than Sheet-L. The different cube texture levels are more obvious in the through-thickness EBSD maps where the grains with cube orientation are highlighted (Fig. 4). It should be mentioned that the EBSD method often gives stronger dominant texture component than the X-ray diffraction method [7].

The tensile behavior is dependent on the direction (Fig. 5). Sheet-L has slightly higher strength and better tensile elongation, but its bendability is worse than Sheet-H, especially after pre-strain (Table 2). When observed in the cross-sections under optical microscope (Fig. 6), Sheet-H shows smooth surface topography after bending with no obvious evidence of macroscopic shear localization, whereas Sheet-L shows much rougher topography with strong shear bands where the cracks were initiated. Fig. 7 shows the pre-electro-polished surface of tensile specimens after 18% stretch under

SEM. Displacements were observed in slip lines, grain boundaries and triple junctions and there are more and deeper displacements in Sheet-L than Sheet-H.

Fig. 8 shows the contour plot of major principle strain at 21% elongation for the low and high cube specimens, indicating a shear band generated for both cases. After the localized necking, most imposed deformation/strain accumulates in this necking region as the loading keeps increasing. Furthermore, the specimen with low cube experiences more severe strain localization and has high strain value from diffusing necking to localized necking transition under loading. This conclusion is consistent with the previous studies by Wu [6,8], which reveals that sheet metal with high cube has better formability than that with less cube.

Fracture is usually initiated near the bend outer surface where the tension is the maximum. The nucleation sites for cracks are the places that local strain is concentrated, such as shear bands and around large second phase particles. In the present work, the different bendability in the two sheets is unlikely due to large particles, since the particle sizes and spatial distributions are similar (Fig. 2). As shown in Fig. 6, upon bending the cracks are initiated in the shear bands near the sheet outer surface. The shear bands are narrow regions with intensive shear localization, and in high-Mg aluminum sheet alloys shear bands may develop across the sheet thickness. Although shear bands are relatively independent of grain structure or crystallographic texture, they are less intensive in high-cube Al-Mg alloy sheets. This is in agreement with the fact that in plain strain tension the strain localization is less intensive in a high-cube sheet than a low-cube one, as observed in SEM and confirmed by FE modeling in the tensile specimens.

4. Summary

The grain structure, texture, tensile properties and bendability of two AA5754-O temper sheets, one with low and another with high cube crystallographic texture, were characterized by various means. It has been demonstrated that the high-cube sheet has better bendability than the low-cube one, especially after pre-strain. This phenomenon is explained by the fact that the cube texture significantly delays the initiation of localized necking under in-plane plane strain tension, and it has been confirmed by FE based rate-dependent single crystal plasticity modeling.

References

[1] M. Pinkham: Aluminum International Today, 16 (2004) 18-19.
[2] W.F. Hosford and R.M. Caddell: Metal Forming: *Mechanics and Metallurgy*, (Prentice Hall, Englewood Cliffs, NJ, 1993) pp. 274.
[3] A.K. Gupta: unpublished work.
[4] P. Van Houtte: *The MTM-FHM Software System*, Version 2, KU Leuven, 2000.
[5] ABAQUS Manual, Version 6.7.
[6] P.D. Wu, D.J. Lloyd, M. Jain, K.W. Neale and Y. Huang: Int. J. Plasticity, 23 (2007) 1084-1104.
[7] H. Jin: Mater. Sci. Tech., in print.
[8] P.D. Wu, K.W. Neale and E. Van der Giessen: Int. J. Plasticity, 12 (1996) 1199-1219.

Table 1. The mean grain size (D) measured in the longitudinal sections by optical microscopy. D_L refers to the grain diameter along the RD, and D_T refers to the grain thickness.

	near surface		centre	
	D_L	D_T	D_L	D_T
Sheet-L	19.1 μm	15.4 μm	27.4 μm	17.9 μm
Sheet-H	17.4 μm	12.7 μm	26.6 μm	16.0 μm

Table 2. The $\dfrac{r}{t}$ value determined in wrap bend test.

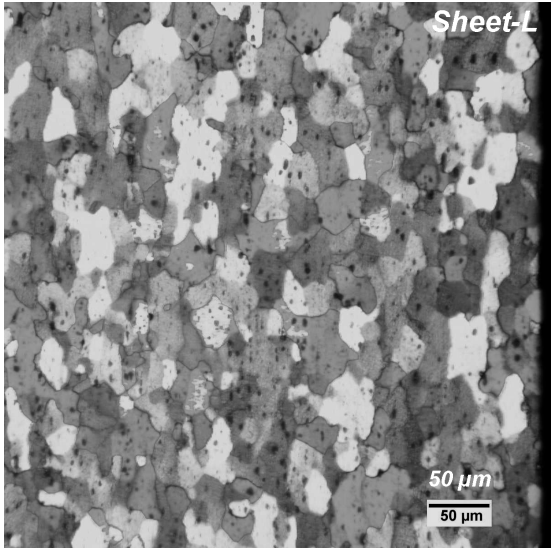|	as-is		pre-strained	
	transverse	longitudinal	transverse	longitudinal
Sheet-L	0.04	0.04	0.7	0.8
Sheet-H	0.04	0.03	0.3	0.1

Fig 1. Optical images taken in the longitudinal sections of the sheets showing the grain structures. The RD is vertical.
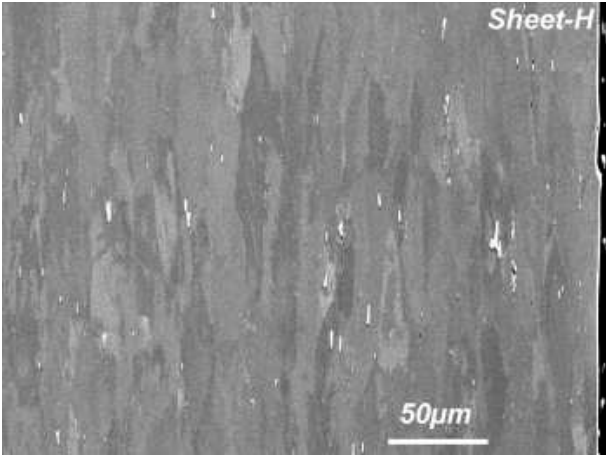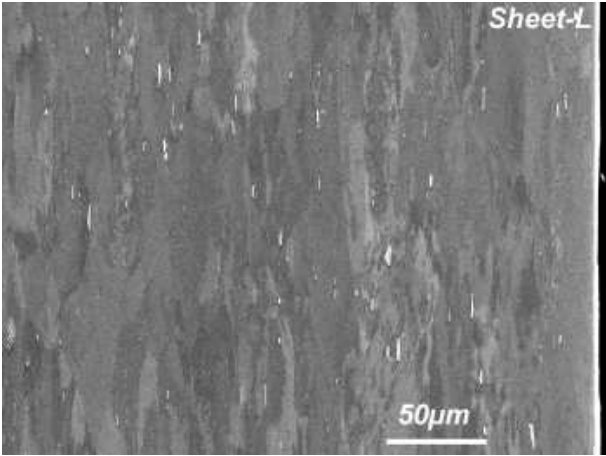

Fig 2. SEM images taken in the longitudinal sections of the pre-strained sheets showing the second phase particles. The RD is vertical.
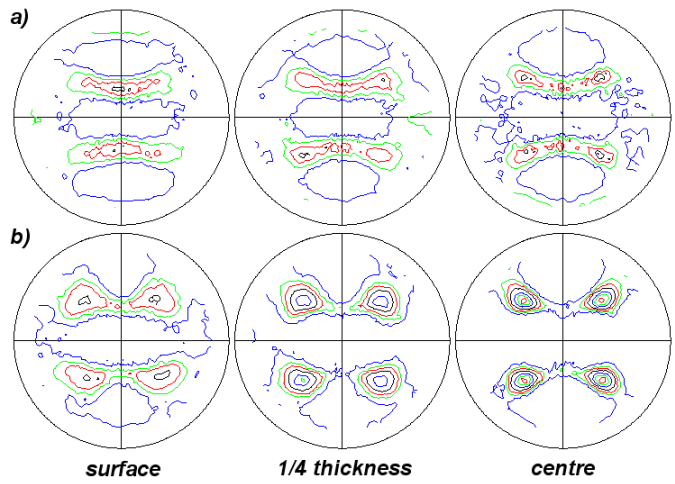
Fig 3. The (111) X-ray pole figures of a) Sheet-L and b) Sheet-H. The contour levels are 1.0, 1.5, 2.0, 3.0, 5.0, 7.0 and 9.0.
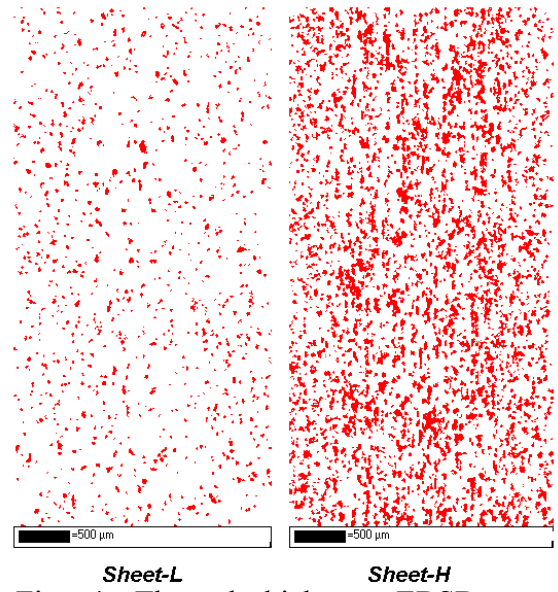
Fig. 4. Through-thickness EBSD maps showing the grains with cube orientation. The RD is vertical.
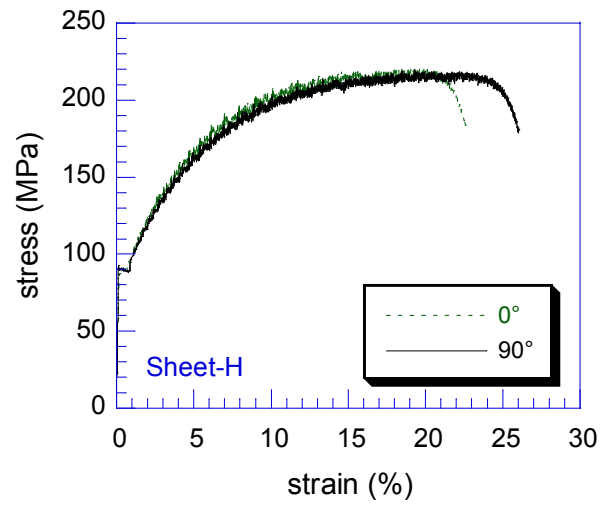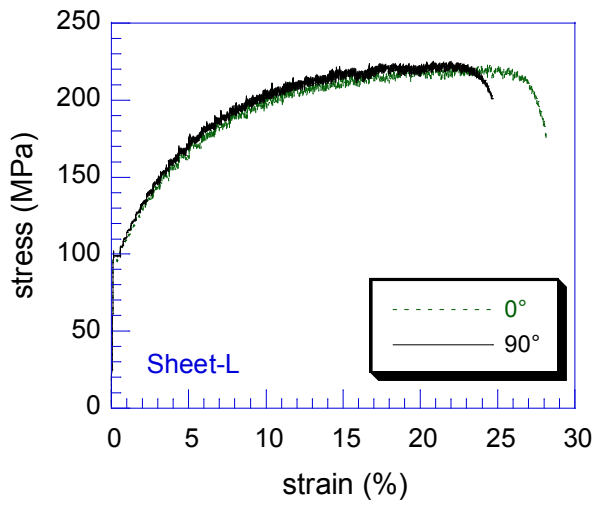

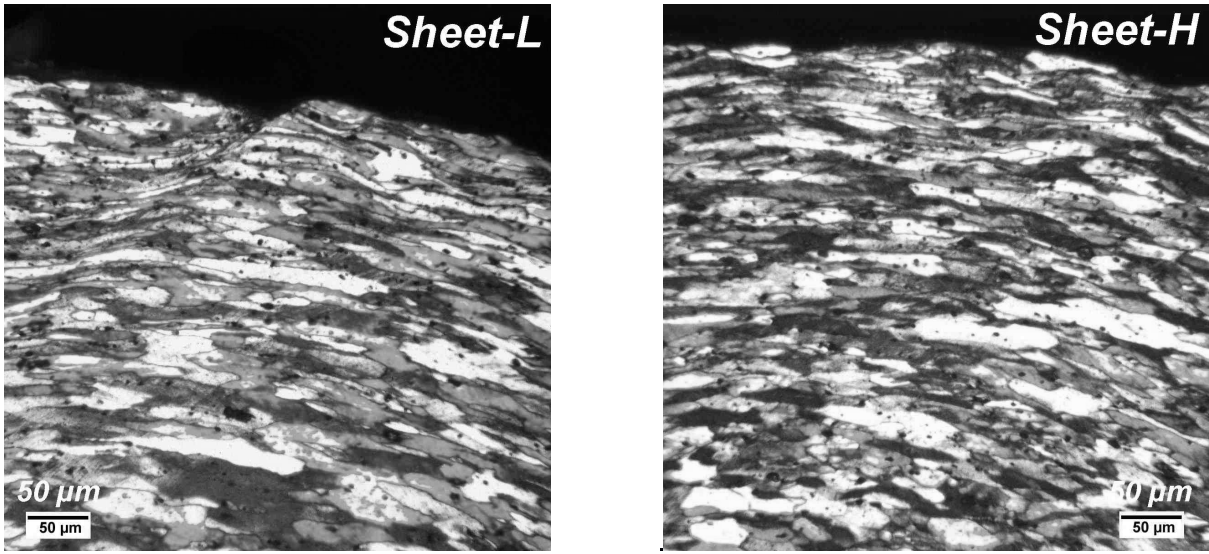Fig. 5. Tensile curves of Sheet-L and Sheet-H.

Fig. 6. Optical images of Sheet-L and Sheet-H after 18% pre-strain and bending test.

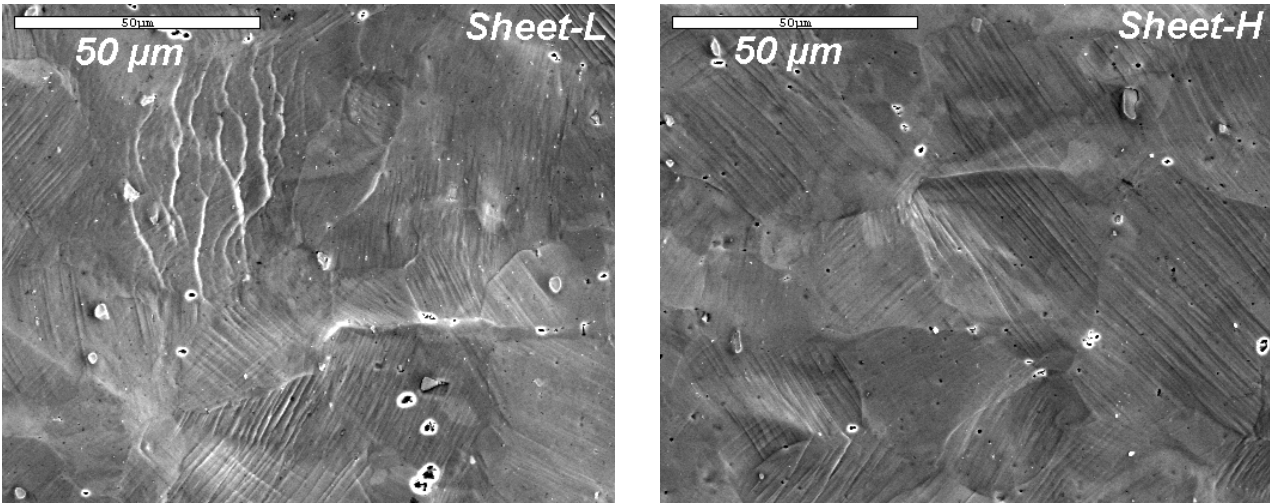Fig. 7. Secondary electron images of Sheet-L and Sheet-H after 18% stretch.

LE, Max. In-Plane Principal
(Ave. Crit.: 75%)
+9.80e-01
+8.71e-01
+7.62e-01
+6.53e-01
+5.44e-01
+4.36e-01
+3.27e-01
+2.18e-01
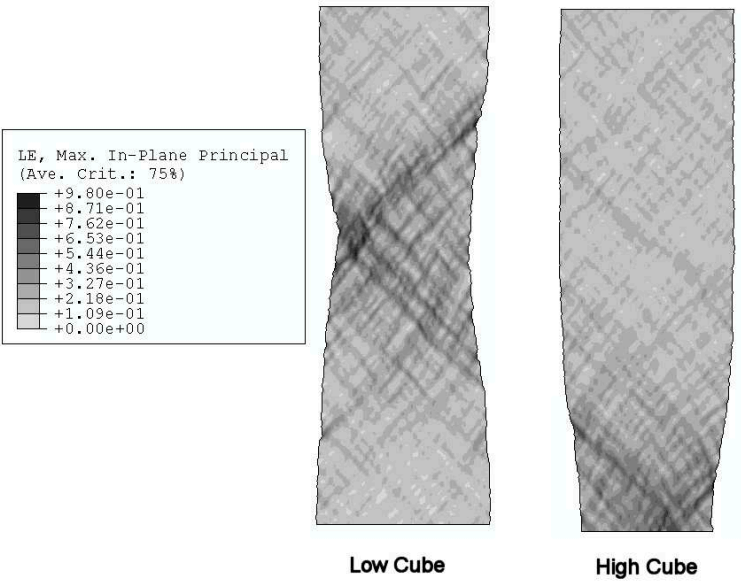+1.09e-01
+0.00e+00

Low Cube   High Cube

Fig. 8. In-plane principle strain in the FE modeling at 21% tensile elongation.